Fish and Shellfish Immunology 86 (2019) 465–473

Contents lists available at ScienceDirect

Fish and Shellfish Immunology

journal homepage: www.elsevier.com/locate/fsi

Full length article

An affinity peptide exerts antiviral activity by strongly binding nervous necrosis virus to block viral entry

Qiong Zhou[a], Jing Zhang[a], Runqing Huang[a], Siyou Huang[a], Yujia Wu[a], Lijie Huang[a], Jianguo He[a,b], Junfeng Xie[a,*]

[a] State Key Laboratory of Biocontrol, Institute of Aquatic Economic Animals and Guangdong Provincial Key Laboratory of Improved Variety Reproduction in Aquatic Economic Animals, School of Life Sciences, Sun Yat-sen University, Guangzhou, China
[b] School of Marine Sciences, Sun Yat-sen University, Guangzhou, China

ARTICLE INFO

Keywords:
Nervous necrosis virus
Phage display peptide library
Affinity peptide
Binding capacity
Antiviral activity

ABSTRACT

Nervous necrosis virus (NNV) causes viral nervous necrosis (VNN), a disease that leads to almost 100% mortality among larvae and juvenile fish, severely affecting the aquaculture industry. VNN vaccines based on inactivated viruses or virus-like particles (VLPs) are unsuitable for fish fry with immature adaptive immune systems. Here, we applied an anti-NNV strategy based on affinity peptides (AFPs). Three phage display peptide libraries were screened against RBS, the VLP of orange-spotted grouper nervous necrosis virus (OGNNV). From the positive clones, a dodecapeptide with the highest binding capacity (BC) to RBS was selected. This AFP agglutinated or disrupted virion particles, inhibiting RBS entry into sea bass (SB) cells. To enhance BC and solubility, we amended the AFP sequence as "LHWDFQSWVPLL" and named as 12C. One to three copies of 12C in tandem were prokaryotically expressed with a maltose binding protein (MBP) linked by a flexible peptide. Of the recombinant proteins expressed, MBP-triple-12C (MBP-T12C) exhibited the highest BC, efficiently blocked RBS entry, and strongly inhibited OGNNV infection at viral entry. Moreover, MBP-T12C bound the VLPs of all NNV serotypes, displaying broad-spectrum anti-NNV ability, and recognized only OGNNV and mud crab virus, demonstrating binding specificity. Therefore, these anti-NNV AFPs specifically bound NNV, aggregating or disrupting the viral particles, to reduce the contact probability between the virus and cell surface, subsequently inhibiting viral infection. Our results not only provided a candidate of anti-NNV AFP, but a framework for the development of antiviral AFP.

1. Introduction

Viral nervous necrosis (VNN), also known as viral encephalopathy and retinopathy (VER), is a serious and highly infectious fish disease that has caused mass mortalities in more than 40 marine [1] and freshwater teleost species [2], primarily at the larval and juvenile stages [3]. VNN causes an infectious neuropathological condition that is characterized by necrosis of the central nervous system, including the brain and retina, which shows clinical signs of abnormal swimming behavior and darkening of the fish skin [4]. VNN is caused by piscine nodaviruses, nervous necrosis viruses (NNVs), that are members of the *Betanodavirus* genus Nodaviridae family [5]. Betanodaviruses are small, spherical, non-enveloped RNA viruses. The bipartite single-stranded (+) RNA genome are encapsulated by 180 molecules of a single self-assembly capsid protein (CP) which is translated from the RNA2 segment [5]. The RNA1 segment of NNV encodes the RNA-dependent RNA polymerase (RdRp) which is responsible for viral genome replication and can trigger type I interferon via interferon regulatory factor 3 in fish cells [6]. The multifunction B2 protein, which antagonizes cellular RNA interference [7], is encoded by a subgenomic RNA (RNA3) transcribed from the 3' end of RNA1 [5].

Betanodaviruses are classified into four genotypes based on the T4 region of RNA2 segment: Tiger puffer nervous necrosis virus (TPNNV), Red-spotted grouper nervous necrosis virus (RGNNV), Barfin flounder nervous necrosis virus (BFNNV) and Striped jack nervous necrosis virus (SJNNV); SJNNV is the type species of *Betanodavirus* [8]. Based on the viral neutralization tests using rabbit anti-NNV sera, these four betanodavirus genotypes are divided into three major serotypes: serotype A (including SJNNV), serotype B (including TPNNV), and serotype C (including BFNNV and RGNNV) [9]. Furthermore, there is no cross-immunoreactivity between serotype A and C, and only partial cross-immunoreactivity between serotype B and C in assay of *in vitro*. In

* Corresponding author. School of Life Sciences, Sun Yat-sen University, Guangzhou, 510006, China.
E-mail address: xiejf@mail.sysu.edu.cn (J. Xie).

https://doi.org/10.1016/j.fsi.2018.12.003
Received 7 August 2018; Received in revised form 25 November 2018; Accepted 1 December 2018
Available online 04 December 2018
1050-4648/

addition, it was shown that the two main betanodavirus species, RGNNV and SJNNV, were confirmed not cross-protective *in vivo* [10]. Therefore, multivalent vaccines against NNV should be produced in order to broaden the range of protection.

However, other antiviral strategies with broader ranges, such as antiviral agents, should also be useful against NNV. Possible antiviral agents include proteins (e.g., antibodies [11] and antimicrobial peptides (AMPs) [12,13]), nucleic acids (e.g., aptamers [14]), and chemical compounds [15]. AMPs, usually 12 to 50 amino acids long with low molecular weights (1–5 kDa), are mostly small, cationic, and amphipathic peptides with broad-spectrum antimicrobial abilities against gram-positive or -negative bacteria, fungi, parasites, and viruses [16]. Many AMPs have been identified in marine teleosts, including epinecidin [17], defensin [18], pleurocidin [19], hepcidin [20,21], cathelicidin [22], piscidin [23,24], cyclic shrimp anti-lipopolysaccharide factor (cSALF) [25], and so on. Some AMPs have demonstrated antiviral activities against aquatic viruses. For example, tilapia hepcidin 1-5 (TH 1–5) and cSALF inhibited NNV entry into culture cells *in vitro* [12], while grouper epinecidin-1 (CP643-1) and TH 1–5 protected medaka from NNV infection *in vivo* [13]. Defensin from orange-spotted grouper [18] and Tachyplesin I from horseshoe crab [26] inhibited the infection and replication of Singapore grouper iridovirus (an iridovirus) and RGNNV (a betanodavirus). It has been elucidated that some AMPs act against NNVs via different mechanisms. AMPs interact directly with certain pathogen components [12,18,26,27], leading to pathogen disruption or agglutination [12]; modulate innate [18,26] and adaptive immune responses [28]; and recruit other cell effectors, such as chemokines [29]. For example, to exert anti-NNV functions, TH 1–5 and cSALF agglutinated and clumped purified NNV particles [12], while CP643-1 induced the expression of antiviral Mx protein in pre-treated cBB cells [13].

It is difficult to obtain an ideal AMP, because AMPs are natural products that are typically identified by complicated means, such as expression differentiation analysis, homologous cloning, and natural products screening. In contrast, it is much simpler to screen for peptides that bind to the pathogen. Affinity peptides (AFPs) is good candidates that exert antiviral activity via binding to pathogens and interfering with viral function in several ways. For example, HIV-1 Gag protein were used to screen a library of M13-derived phages presenting random 12-mer peptides at the N terminus of their pIII coat protein [30]. This phage display biopanning identified a novel 12-mer peptide, capsid assembly inhibitor (CAI), which binds Gag and inhibits the assembly of immature- and mature-like capsid particles *in vitro*.

In this study, VLP of orange-spotted grouper nervous necrosis virus (OGNNV), RBS, was used as a target for screening with two phage display peptide libraries and three clones were obtained. Based on a binding assay and bioinformatics comparison, we identified and chemically synthesized a 12-mer peptide with a high binding capacity (BC) for RBS. Moreover, the selected peptide was modified to be multiple copies in tandem blanking with flexible peptide and was prokaryotically expressed as a recombinant protein to increase the BC and reduce production cost. The binding pattern of the peptide and protein were examined, and the anti-NNV mechanisms were also elucidated *in vitro*.

2. Materials and methods

2.1. Virus and cells

The SB fibroblast cell line derived from *Lates calcarifer* larvae was obtained from Temasek Life Sciences Laboratory of the National University of Singapore [31]. SB were used for the cell entry assay of VLP and were grown in minimal essential medium (MEM, Gibco, USA) supplemented with 10% fetal bovine serum (FBS, Gibco). Striped snake head cell (SSN-1) sub-clone No.1 (SC1) cell line, which was established from SSN-1 cell line, was maintained in L-15 medium at 27 °C. OGNNV was isolated from moribund orange-spotted grouper larvae collected in HaiNan province of China, propagated, and titrated in SC1 cells. To perform NNV titer assay, the supernatants of SC1 cells infected with OGNNV of indicated days were diluted from 10^{-1} to 10^{-8} and used to infect fresh SC1 cells with 8 repetitions per dilution. After five days of culture, the well numbers of infected cell of each dilution were identified by cytopathic effect. $TCID_{50}$ was calculated by Reed-Muench method [6].

2.2. Phage display peptide library screen

Two M13 phage library (Ph.D.-12 and Ph.D.-7, New England Biolabs, USA) encoding random linear 12-mer or 7-mer peptides at the N-terminus of their pIII coat protein was used. Surface panning procedure was used as described in the manual. Briefly, 150 μL of the purified RBS (100 μg/mL) were coated with coating buffer (0.1 M $NaHCO_3$, pH 8.6) in each well of the 96-well plate and the following procedures were independently for Ph.D.-12 and Ph.D.-7. After blocking with BSA (5 mg/mL) in coating buffer and washing 5 times with 0.1% TBST (50 mM Tris-HCl, 150 mM NaCl, 0.1% [v/v] Tween-20, pH 7.5), the well containing RBS was incubated with 100 μL of diluted library (5×10^{11} sequences) for 1 h at room temperature. After washed 10 times with TBST, bound phages were eluted with elution buffer (0.2 M glycine, 1 mg/mL BSA, pH 2.2) and neutralized with 1 M Tris (pH 9.1). Eluates were incubated with *Escherichia coli* ER2738 cells and amplified for 5 h at 37 °C. The amplified phages were collected, purified, and titrated for the next round of surface panning procedure. After 3 rounds of panning, the phages were used for additional negative and positive selection. The selected phage DNA was prepared. The region of interest was amplified and sequenced with M13KE-F and the supplied −96 gIII sequencing primer (Table S1).

2.3. Peptides and proteins

Peptides (7-mer and 12-mer) including positive, negative control (NC), and modified sequence (Table 1) were obtained as lyophilized trifluoroacetic acid salts (GL Biochem, China). To generate multiple tandem 12C, including D12C and T12C, DNA templates of 12C, D12C, and T12C with flexible sequence, GGGGS, between each 12C were synthesized (Sangon Biotech, China) and amplified by primers indicated in Table S1. The amplified products with correct size were cloned into *Eco*R I and *Hin*d III sites of pMal-C2 which is expressing maltose-binding protein (MBP) fusion protein (NEB, USA). MBP-12C, MBP-D12C, and MBP-T12C were expressed in *E. coli* BL21(DE3) containing the recombinant plasmids, verified by western blot using rabbit anti-MBP polyclonal antibody (NEB, USA), and purified by Amylose resin (NEB, USA). The concentrations of the purified proteins were determined by SDS-PAGE and BCA protein assay kit (Beyotime, China).

Table 1
Sequences of the selected phage clones and peptides for chemical synthesized.

Name	Sequence (N−C)	From	Number of repetitions
7–1	KVWILPA	PhD-7	6/30
7–2	KVWVIPS	PhD-7	4/30
7-18(NC[a])	APTEHWA	PhD-7	1/30
12-1(12A[b])	VHWDFRQWWQPS	PhD-12	11/30
12-2(NC)	AFKHGMQTMPPL	PhD-12	1/30
12B	KHWDFRQWWQPS	12A	–
12C	LHWDFQSWVPLL	Grouper gene[c]	–

[a] NC = negative control. One non-consensus sequence was randomly selected from each library as NC in the following experiment.

[b] 12-1 was the name of the phage clone and 12A was the corresponding peptide synthesized by chemical method.

[c] 12C is the homologous sequence from ANK-GPCR protein of orange-spotted grouper.

RBS, different serotype VLPs, and CP mutants were produced in *E. coli*. RBS was expressed by modified pQE30 (Qiagen) containing full-length *cp* gene of OGNNV (GenBank: AF534998) in M15 as described [31]. Full-length *cp* genes of SJNNV (AB056572), BFNNV (EU236147), and TPNNV (EU236149) were synthesized by Sangon Biotech (China), amplified with primers indicated in Table S1, and inserted into pRSETA at *Hin*d III and *Xba* I sites. The recombinant plasmids were expressed in BL21(DE3). For SJNNV VLP (SJVLP), TPNNV VLP (TPVLP), or BFNNV VLP (BFVLP) expression, the subcultures ($O.D._{600} \approx 0.4$) of recombinant bacteria were cooled down to 16 °C, 23 °C, or 30 °C, added IPTG to final concentrations of 0.4 mM, 0.3 mM, or 0.5 mM, and induced to express for 12 h, 12 h, or 5 h. All VLPs were purified by gradient centrifuge, verified the purities by SDS-PAGE, and confirmed the particle structure by electron microscopy as described [32]. Two parts of *cp* gene, 1–624 bp or 625–1017 bp representing 1–209 aa (N domain) or 210–338 aa (C domain) of CP, were amplified with primers indicated in Table S1, inserted into pRSETA-GFP (gfp was already inserted into *Bgl* II and *Kpn* I sites) at indicated restriction sites, and expressed as N-terminal fused GFP recombinant proteins in BL21(DE3) to generate GN and GC, respectively. GN and GC cannot generate particle structures due to the interference of the fused GFP, representing the non-particle proteins of OGNNV CP.

2.4. SDS-PAGE and western blot

Cells or bacteria were lysed in lysis buffer. The lysate was centrifugated in 15,000 × *g* for 20 min at 4 °C. The supernatant and the pellet were collected and an aliquot of 30 μg total protein was subjected to SDS-PAGE analysis. Resolved proteins were transferred to a nitrocellulose membrane (Millipore, USA). The membranes were blocked with 10% skim milk for 1 h at room temperature, and then probed with anti-RBS (polyclonal antibody produced in mouse, total immunoglobulin), anti-MBP, anti-GFP or anti-β-actin antibodies (Sigma, Germany) as indicated for 2 h. After washed with PBST (0.5% Tween-20 in PBS) for four times, the membranes were incubated with goat anti-mouse-HRP antibody (1:5000, Santa Cruz, USA) for 1 h. After four times of washing, protein bands were detected by enhanced chemiluminescence (ThermoFisher, USA) via a chemiluminescence instrument Tanon-5200 (China). For in-cell RBS semi quantitation, the band intensity of RBS was normalized with that of the corresponding β-actin. The normalized ratio of NC was arbitrarily set as 1, and used in the calculation of entry efficiency (percentage) in other samples.

2.5. Transmission electron microscope (TEM)

The purified RBS (1 μg/μL) was respectively mixed with the same volume of 12B (0.4 or 4 μg/μL), 12NC (4 μg/μL), sterilized water or anti-RBS sera (1 μg/μL), and incubated at 28 °C for 12 h. The shape, size and integrity of the RBS in the mixtures were confirmed by the negative staining with 1% phosphotungstic acid and TEM (JEOL JEM-1400, Japan) observation.

2.6. Enzyme-linked immunosorbent assay (ELISA)

For phage binding with RBS, 10 μg RBS was coated overnight in each well of 96-well microtiter plate with 100 μL coating buffer (0.015 M Na_2CO_3, 0.035 M $NaHCO_3$, pH 9.6) and blocked with BSA (5 mg/mL) in coating buffer for 1 h at room temperature. After washed with 0.5% TBST for 3 times, the selected phages amplified from single plaques with different titers were added and incubated for 1 h at 26 °C. After washed with 0.5% TBST for 3 times, bound phages were detected with a monoclonal antibody, anti-M13-horseradish peroxidase (HRP) conjugate (GE Healthcare, 1:5000 in wash buffer). ELISAs were developed using standard procedures.

For peptide binding with RBS, in-direct ELISA was used. One hundred microliter of chemical synthesized peptides in different concentrations were coated in each well (the coating buffer contains 20% acetonitrile when 12A or 12C was used), blocked, and washed. RBS (20 μg/mL, 100 μL for each well) was incubated with washed peptides for 1 h at 26 °C. After washed with 0.5% TBST for 3 times, RBS was detected with primary antibodies, mouse anti-RBS sera (1:6000 in wash buffer), and secondary antibody, goat anti-mouse-HRP conjugate (1:8000 in wash buffer, Bioworld, China). ELISAs were developed using standard procedures. For electrostatic force determination assay, 100 μL of 12B (40 μg/mL) was coated in each well, different concentrations of NaCl were added spontaneously with RBS for binding, and other procedures were the same as described above.

For MBP-fused protein binding with RBS, RBS was coated, blocked, and incubated with purified MBP-12C, MBP-D12C or MBP-T12C in different concentrations. Bound proteins were detected with anti-MBP-HRP antibody (1:10,000 in wash buffer). Other procedures were the same as described above.

For broad-spectrum binding assay, 100 μL of RBS, SJVLP, TPVLP, BFVLP, GN, and GC (60 μg/mL each) were coated in each well respectively and other procedures were the same as described above. For binding specificity assay, high titer viral stocks of 12 aquatic viruses including 9 fish viruses: OGNNV, tiger frog virus (TFV), mandarin ranavirus-GD1301 (MRV) [33], infectious spleen and kidney necrosis virus (ISKNV), rock bream iridovirus (RBIV), grouper iridovirus (GIV) [34], *Siniperca chuatsi* rhabdovirus (SCRV), Hirame rhabdovirus (HIRRV), Koi herpesvirus (KHV) [35]; 2 crab viruses: mud crab reovirus (MCRV) [36], mud crab virus (MCV) [37]; and 1 shrimp virus: white spot syndrome virus (WSSV) [38] were selected. All the piscine viruses were propagated on culturing cell lines *in vitro* and diluted to 10^5 $TCID_{50}$/0.1 mL for ELISA. There is no cell line can support the infection and replication of MCRV, MCV, and WSSV. Therefore, genome copies were used to indicate the viral concentration. MCRV, MCV, and WSSV were diluted to 10^5 copies/g body weight in 0.1 mL from the viral stocks. All viruses were coated in each well respectively, blocked, washed, and incubated with purified MBP-T12C (40 μg/mL). Bound proteins were detected with anti-MBP-HRP antibody (1:10,000 in wash buffer). Other procedures were the same as described above.

For detection of inhibition efficiency of RBS entry into SB cells, the quantities of intracellular RBS were determined by ELISA after the cell entry assay and endogenous β-actin was used as an internal normalization control. In a 96-well plate, 300 μL of 30-fold diluted lysate for RBS detection or 100-fold diluted lysate for β-actin detection were coated equally in three wells. Primary antibodies of anti-RBS and mouse anti-β-actin (Santa Cruz, USA) were used and other procedures were the same as described above.

2.7. Cytotoxicity assay

SB cells grown in 96-well plates were incubated with the MBP-T12C at different concentrations (50, 100, 200, 300, 400, and 500 μg/mL) for 48 h. Then cell viability was assayed using CellTiter 96® Aqueous One Solution Cell Proliferation Assay (Promega, USA) according to the manufacturer's instructions.

2.8. Cell entry assay

For peptide inhibition of RBS entry, 12B, 12NC, anti-RBS sera, and PBS (NC) were mixed with RBS (0.01 μg/μL) in equal volume for 1 h, respectively. The mixtures were incubated with fresh SB cells (80% confluence) in 12-well plates for 2 h to perform RBS entry. The treated cells were washed twice with cold PBS, harvested, and lysed in RIPA lysis (Beyotime, China) buffer on ice for 30 min. The lysate was centrifugated in 15,000 × *g* for 20 min at 4 °C. The supernatant was collected and an aliquot of 30 μg total protein was subjected to SDS-PAGE and semi quantitation western blot analysis.

For MBP-T12C inhibition of RBS entry, different concentrations of MBP-T12C or PBS were mixed with equal volume of RBS (60 μg/mL) for

1 h at room temperature, and then the mixtures were incubated with SB cells (80% confluence) that were seeded on coverslips in 12-well plates for immunofluorescence assay (IFA) or 96-well plates for ELISA. After incubated for 2 h, SB cells in 12-well plates were washed twice with PBS, fixed with 4% paraformaldehyde for 15 min, permeated with 0.2% Triton X-100 for 10 min, and then blocked with 5% BSA for 1 h. Cells were incubated at 4 °C overnight with primary antibody, anti-RBS sera (1:1000 in PBS). Subsequently cells were washed three times with PBS for 15 min and incubated for 1 h at room temperature with secondary antibody, Alexa Fluor 488 donkey anti-mouse IgG (1:4000 in PBS, Invitrogen, USA). Cell nuclei were labeled with Hoechst 33342 (1:1000 in PBS, Invitrogen, USA) for 10 min, and then cells were washed three times with PBS and added with ProLong™ Gold antifade mountant (Invitrogen, USA). A fluorescent inverted microscope (Nikon Eclipse Ti−U, Japan) was used to acquire images utilizing Nikon NIS Elements imaging software (Br2 v3.21). Six wells of SB cells in 96-well plates with entered RBS were washed twice with PBS, lysed with 20 μL of lysis buffer in each well, and combined as one sample for ELISA. The entry efficiency was generated as the percentage of the RBS quantities in MBP-T12C treated cells relative to that of PBS treated cells. The entry efficiency of PBS treated cells was arbitrarily set as 100%. The data shown are the mean ± SD of the results from three independent experiments. Statistical differences of RBS content from different concentrations were assessed by paired Student's t tests. Numerical results are presented as mean ± SD with 95% confidence intervals and $p < 0.05$ was considered statistically significant (*, $p < 0.05$; **, $p < 0.01$).

2.9. NNV neutralization assay

OGNNV was respectively diluted to 10^4, 10^5, and 10^6 $TCID_{50}$/mL, mixed with different concentrations of MBP-T12C or PBS in medium to total volume of 100 μL (each well) for a well of 96-well plate or 1 mL for a well of 12-well plate at room temperature for 2 h, and incubated with SC1 cells (90% confluence). For samples from 96-well plates at 12, 24, and 36 h post-infection (hpi), supernatants were collected for CP detection by ELISA and infected cells were lysed for RNA extraction and subsequent reverse transcription quantitative PCR (RT-qPCR). For samples from 24-well plates at the same indicated time points, the infected cells were fixed for IFA.

2.10. RT-qPCR

Total RNA was isolated from different groups of infected SC1 cells using the RNeasy Mini Kit (Qiagen, Germany), treated with gDNA Eraser, and reverse-transcribed into cDNA using the First Strand cDNA Synthesis Kit (Toyobo, Japan) according to the manufacturer's instructions. Expressions levels of *cp* gene (Table S1) were determined by the Perfect Real-Time SYBR Green Master Mix Kit (Takara, Japan) following the manufacturer's instructions using Light Cycler 480 real-time PCR system (Roche, Switzerland). The PCR conditions were as follows: 95 °C for 1 min, followed by 40 cycles of 95 °C for 10 s, 60 °C for 15 s and 70 °C for 10 s 18S rRNA (Table S1) was used as reference gene.

3. Results

3.1. Phage library screen against OGNNV VLP

To identify the candidate peptides that interact with OGNNV, we screened a phage display random heptapeptide library (PhD-7) and a dodecapeptide library (PhD-12) using the VLP of OGNNV (RBS) as the target molecule. After three rounds of surface panning, titerings were carried out (Fig. S1A), and thirty clones from each library were selected for PCR verification and sequencing. PCR verified 30 positive clones (Fig. S1B) and we selected 3 sequences with 6, 4, and 1 repetitions from PhD-7 library. While from PhD-12 library, there were 27 positive clones

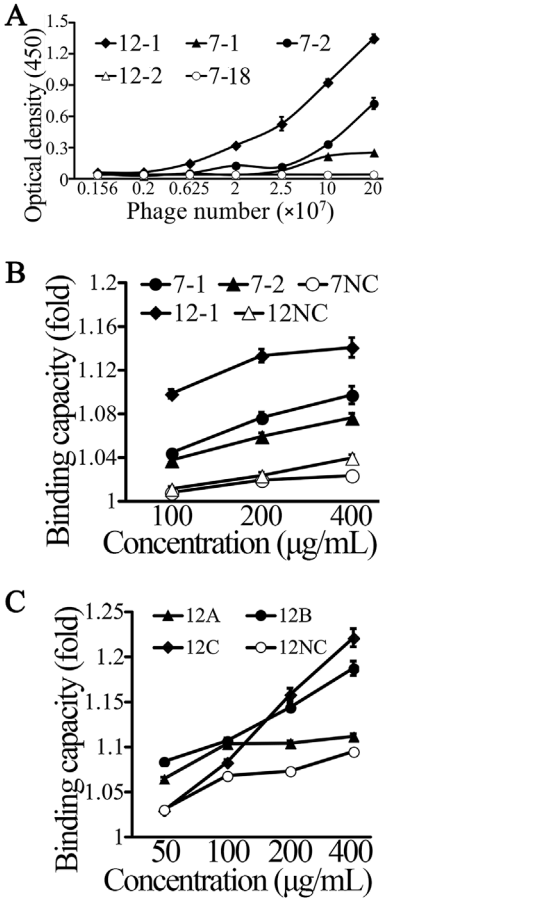

Fig. 1. Screen of phage clones and AFPs binding with RBS. (A) Ph.D.™-7 and 12 phage display peptide libraries were screened against RBS. One dodecapeptide (12-1) and two heptapeptides (7-1 and 7-2) were obtained, and the bindings to RBS were specific and dose-dependent (from 0.156 to 20×10^7 clones) as comparing with, the negative controls, the random selected phage clones (12-2 and 7–18). (B) The peptides from screened out phage clones were chemical synthesized and the BCs were dose-dependent (from 100 to 400 μg/mL) as comparing with the negative control (12-NC and 7-NC). (C) BCs comparation between 12A, 12B, and 12C. The ELISA in (B) and (C) were conducted with coating buffer containing 20% acetonitrile.

verified (Fig. S1C) and 2 sequence with 11 and 1 repetitions was screened out (Table 1). To confirm the BC, the selected phage clones, 7-1, 7-2, 7–18, 12-1, and 12-2, were amplified and diluted to different concentrations to test against RBS using ELISA. The phage clones 12-1, 7-1, and 7-2 efficiently bound RBS in dose-dependent manner, with clone 12-1 exhibiting the greatest BC (Fig. 1A). In contrast, the phage clones 7–18 and 12-2 did not bind RBS and were therefore used as negative controls (NCs).

To evaluate peptide performance, the 5 selected phage clones were sequenced, and the corresponding peptides were chemically synthesized and purified. An indirect ELISA indicated that the AFP of 12-1 (12A) had the highest BC for RBS of all the selected peptides (Fig. 1B). Therefore, 12A was selected for the subsequent experiments. However, 12A was hardly soluble in water. Thus, in the indirect ELISA, its BC for RBS was tested in coating buffer containing 20% acetonitrile.

To increase the solubility of 12A, its amino acid sequence was amended with the fragment “KHWDFRQWWQPS”. This modified peptide is referred to herein as 12B. At the same time, 12A was used to blast against the transcriptome of the orange-spotted grouper, and a protein with homologous sequence to 12A was identified. The protein is designated as ankyrin repeat domain-containing protein 13C-A-like and GPCR-chaperone (ANK-GPCR), and the sequence homologous to 12A

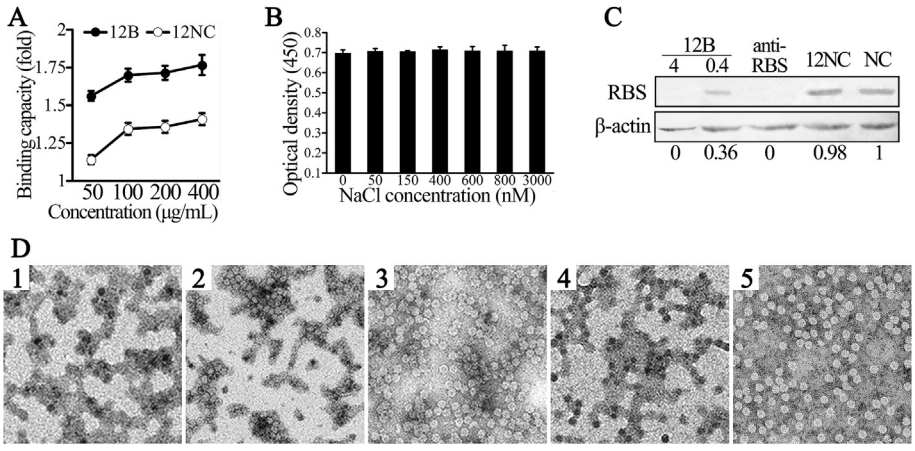

Fig. 2. Binding mechanism of 12B with RBS. (A) The BC of 12B in PBS was significant higher than that of the negative control (12NC) detected by ELISA. (B) 12B bound RBS in different concentration of NaCl detected by ELISA. The binding of 12B is not dependent on electrostatic force. (C) 12B inhibited the entry of RBS. Different concentrations (4 and 0.4 μg/μL) of 12B were incubated with RBS for 1 h and RBS entry was performed subsequently. High concentration of 12NC (4 μg/μL) and non-treated cells (NC) were served as controls. Western blot was performed to detected the in-cell CP and β-actin, which was served as internal control. Each entry efficiency, which generated by normalizing the CP level of each sample to that of NC, was listed under figure. (D) TEM observation of AFPs treated RBS. High concentration of 12B (panel 1, 4 μg/μL) disrupted the 3D structure of RBS as the anti-RBS polyclonal antibody did (panel 4, 1 μg/μL). Low concentration of 12B (panel 2, 0.4 μg/μL) mediated the aggregation of RBS. 12NC cannot interfere RBS even in high concentration (panel 3, 4 μg/μL), and the dispersion of the 12NC-treated sample was the same as untreated control (panel 5).

was "LHWDFQSWVPLL", referring to as 12C. However, the solubility of 12C was similar to that of 12A. Therefore, we compared the BC for RBS among the three AFPs (12A, 12B, and 12C) using indirect ELISA with 20% acetonitrile. As shown in Fig. 1C and 12C was demonstrated the highest BC for RBS at high concentrations (> 20 μg) although the background O.D. reads were high. Nevertheless, we should use other strategy to enhance the solubility of 12C in order to apply the anti-NNV ability of 12C.

3.2. 12B inhibited RBS entry by agglutinating virions

To determine the BC of the selected AFP for RBS, the soluble chemical synthesized 12B was tested in an ELISA under normal conditions. As Fig. 2A shown, 12B efficiently bound RBS in dose-dependent manner. Furthermore, we attempted to interfere with the binding by adding NaCl to the ELISA in increasing concentrations. We found that the binding of 12B to RBS is not dependent on electrostatic force, as the BC did not alter even at high concentrations of NaCl (Fig. 2B). This indicated that other mechanisms, besides electrostatic forces, might be involved in the binding between 12B and RBS. In addition, this result implied that 12B might be used in high salinity environments, such as sea water.

To examine whether 12B restricted RBS entry, we performed entry inhibition experiments using the RBS-SB cell entry model. Then western blots were used to detect in-cell CP levels. As shown in Fig. 2C, high concentration of 12NC (4 μg/μL) did not reduce RBS entry (entry efficiency = 98%), and the level of in-cell CP was similar to that of NC (entry efficiency was arbitrarily set to 100%). However, low concentration of 12B (0.4 μg/μL) reduced RBS entry efficiency by almost 60% (entry efficiency = 36%), while high concentration of 12B (4 μg/μL) completely inhibited RBS entry, equivalent to1 μg/μL of the polyclonal antibody against RBS (anti-RBS).

To investigate the mechanisms by which 12B inhibited RBS entry, purified RBS was mixed with different concentrations of 12B, anti-RBS, and 12NC for 1 h. Each mixture was then examined with TEM. As Fig. 2D indicated, TEM images showed that 4 μg/μL of 12B (panel 1) agglutinated RBS and disrupted the highly structured virions. The similar effect was observed when 1 μg/μL of anti-RBS was mixed with RBS (Fig. 2D, panel 4). When mixed with low concentration (0.4 μg/μL) of 12B, RBS particles were aggregated but not disrupted (Fig. 2D, panel 2). As control, 12NC, even at high concentration (4 μg/μL), neither aggregated nor disrupted RBS. The appearance of RBS mixed with 12NC was similar to that of intact RBS (Fig. 2D, panel 5). These results suggested that 12B inhibits RBS entry by strongly binding with RBS, and subsequently agglutinating or disrupting RBS particles.

3.3. Construction and expression of recombinant proteins of tandem 12C, VLPs of all serotypes, and CP mutants without 3D structure

Of these three chemical synthesized AFPs, 12C had the strongest BC for RBS, but it is also hardly soluble. Therefore, we used prokaryotic expression instead of chemical synthesis for this AFP. To enhance the BC of 12C, we linked two or three 12C copies in tandem. To avoid the steric hindrance, each 12C was separated by a short flexible sequence, GGGGS (G4S) (Table S1). We also selected maltose-binding protein (MBP) as the fusion tag because this molecule greatly increases solubility of the fusion protein. MBP was fused with one 12C, double 12C (D12C), or triple 12C (T12C) at carbon terminal to generate recombinant proteins, MBP-12C, MBP-D12C, and MBP-T12C. Between MBP and the AFPs, there was also a G4S flexible sequence. The recombinant proteins were expressed, purified (Fig. 3A SDS-PAGE panel), confirmed (Fig. 3A IB panel), and stored for future use.

In *Betanodavirus* genus, four genotypes of viruses correspond to three serotypes. To evaluate the broad-spectrum inhibition of the peptides to most, if not all, of the betanodaviruses, we synthesized the *cp* gene of the other three betanodavirus genotypes. All the *cp* genes were cloned, optimally expressed (Fig. 3B, SDS-PAGE panel), and purified using VLP purification standard procedures. TEM observation verified that all purified products were highly structured VLPs (Fig. 3B, EM panel). Thus, we obtained four genotypes of VLPs across the three serotypes: SJNNV VLP (SJVLP, serotype A), TPNNV VLP (TPVLP, serotype B), BFNNV VLP (BFVLP, serotype C), and RBS (serotype C). However, in Western blots using the anti-RBS polyclonal antibody, TVLP (serotype B) could not be detected, and SVLP (serotype A) had a very weak but detectable band. As belonging to serotype C, BVLP was easily detected by anti-RBS in Western blot (Fig. 3B, IB panel).

In addition to different serotypes VLPs, we also constructed CP mutants based on different segments to evaluate the BC of MBP-T12C for these unstructured monomer proteins. CP amino acid 1–208, including the N and S domains, were fused to the C-terminal of GFP and expressed as a fusion protein (GN). CP amino acid 209–338, including the P domain, were also fused with GFP to be recombinant protein (GC). GN and GC were expressed, purified, and verified (Fig. 3C). These VLPs and monomer proteins were useful as broad-spectrum interaction targets for the screening of anti-betanodavirus reagents.

3.4. The binding properties of MBP-T12C

We then tested the BC of the MBP-fusion proteins for RBS by ELISA. In each well of a 96-well plate, 6 μg of RBS was coated, and different concentrations of the fusion proteins were added. As shown in Fig. 4A, all the fusion proteins bound RBS while the binding curves of MBP-

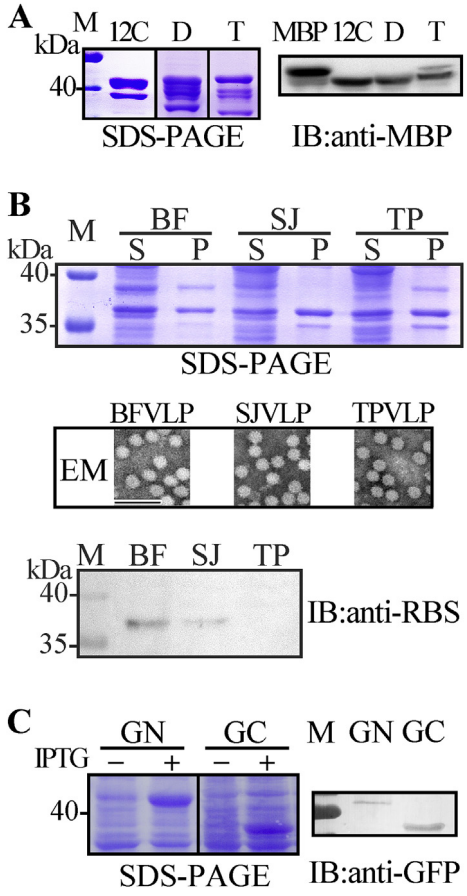

Fig. 3. Expression and identification of MBP fusion proteins, different serotypes VLPs, and CP mutants. (A) MBP fusion protein identification. MBP-12C (12C), MBP-D12C (D), and MBP-T12C (T) were expressed, purified, and identified by SDS-PAGE (left panel) and western blot (right panel). (B) Different serotypes VLPs identification. BFVLP, SJVLP, and TPVLP were expressed in supernatant (S), purified by ultracentrifugation, and verified the particle structure by EM. Anti-RBS sera were used to detect these VLPs while TPVLP (TP) cannot be detected. (C) CP mutants identification. GN and GC were expressed, purified, and identified by SDS-PAGE (left panel) and western blot (right panel).

D12C and MBP-T12C plateaued at 10 μg/mL. This result indicated that the tandem repeats of 12C were highly effective. The BC of MBP-T12C was 9 times of that of MBP-12C and twice that of MBP-D12C at 10 μg/mL. As the BC of 12C was increased by usage of triple tandem repeats and the solubility of 12C was increased by prokaryotic expression with MBP, MBP-T12C was used in the following experiments.

To evaluate the broad-spectrum binding of MBP-T12C, four genotypes of betanodaviruses and two CP mutants were used as targets. The BC of MBP-T12C for RBS, SJVLP, TPVLP, BFVLP, GN, and GC were evaluated by ELISA. We found that, although MBP-T12C bound all these target proteins, the BC of MBP-T12C for TPVLP was the weakest, which was similar to the BC of the anti-RBS antibody (Fig. 4B). Interestingly, MBP-T12C showed the highest affinity for GN. Although GN was probably as a polymer, it was certainly not a highly structured virion particle like RBS. The BC of MBP-T12C for GC was weaker than those for GN and RBS, indicating that the 12C binding sites may be clustered in the N + S domain of CP. These results also implied that the immunogenicity of the CP N + S domain of was stronger than that of the CP P domain in betanodaviruses, and that the N + S domain was more easily bound by AFPs. MBP-T12C had a high affinity for all betanodavirus genotypes.

Besides broad-spectrum BC, we also evaluated the binding specificity of MBP-T12C. In addition to OGNNV, we performed ELISA to tested the BC of MBP-T12C for 11 aquatic viruses, including 8 fish viruses: tiger frog virus (TFV), mandarin ranavirus-GD1301 (MRV) [33], infectious spleen and kidney necrosis virus (ISKNV), rock bream iridovirus (RBIV), grouper iridovirus (GIV) [34], *Siniperca chuatsi* rhabdovirus (SCRV), Hirame rhabdovirus (HIRRV), Koi herpesvirus (KHV) [35]; 2 crab viruses: mud crab reovirus (MCRV) [36], mud crab virus (MCV) [37]; and 1 shrimp virus: white spot syndrome virus (WSSV) [38]. As shown in Fig. 4C, only OGNNV and MCV were obtained the positive signals, indicating that MBP-T12C not only specifically bound betanodaviruses but also interacted with MCV. The capsid sequence of MCV, a newly emergent RNA virus infecting mud crabs, is highly similar to that of nodaviruses that infect shrimps [37]. However, the BC of MBP-T12C for MCV was not dose-dependent (Fig. 4D), suggesting that the binding ratios and binding mechanisms between MBP-T21C and MCV require further study.

3.5. Inhibition of RBS entry by MBP-T12C

The RBS-SB cell model is a well-established system that is ideal for investigations of viral entry mechanisms, entry receptors, and important cell surface components [39]. In this model, the native virus is replaced by RBS, which can be used in high concentrations, is easily detected rapidly after entry, and includes only the viral structure protein, avoiding the interference of the viral genome [39]. First, a cytotoxicity assay was performed to evaluate the influence of high concentrations of MBP-T12C on cells. As shown in Fig. 5A, the MTT assay demonstrated that MBP-T12C did not harm SB cells even at high concentrations (up to 500 μg/mL).

To test whether MBP-T12C inhibited the entry of RBS, we performed the entry inhibition assay. Different concentrations of MBP-T12C were mixed with RBS (60 μg/mL) for 1 h, and then these mixtures were incubated with SB cells for 2 h. RBS entry was detected by IFA (Fig. 5B). MBP-T12C inhibited RBS entry in a dose-dependent manner. Little RBS had entered the cells at 500 μg/mL of MBP-T12C, indicating that RBS entry was strongly inhibited. The entered RBS were also quantified by ELISA. We found that 400 μg/mL of MBP-T12C significantly reduced RBS entry ($p < 0.01$, Fig. 5C).

3.6. OGNNV neutralization by MBP-T12C

To determine the neutralization capacity to native virus, MBP-T12C was diluted to 500 μg/mL and mixed with a different titers of OGNNV (10^4, 10^5, and 10^6 $TCID_{50}$/mL). These neutralization mixtures were incubated with SC1 cells without removal to determine the neutralization capacity and the replication inhibition ability of MBP-T12C. Viral replication in high titer (10^6 $TCID_{50}$/mL) infected SC1 cells was detected by IFA at 12, 24, and 36 hpi (Fig. 6A). The CP signals of MBP-T12C-treated OGNNV at 12 hpi were much lower than those of the untreated virus, indicating MBP-T12C neutralized OGNNV effectively. Similar results were observed at 24 and 36 hpi. The quantification of viral gene level using RT-qPCR (Fig. 6B) and viral protein level using ELISA (Fig. 6C) showed that the neutralized virus was significantly inhibited at 24 and 36 hpi ($p < 0.001$, Fig. 6B left panel; $p < 0.01$, Fig. 6C left panel) comparing with the untreated OGNNV. However, the propagation trends of the neutralized virus in both RNA and protein level were similar with that of the untreated virus. Thus, MBP-T12C probably did not interfere with the replication of high titer OGNNV, but instead bound with the virions at viral entry step to exert antiviral activity. When low titer viral infections (10^4 and 10^5 $TCID_{50}$/mL) were used, MBP-T12C significantly inhibit OGNNV replication in all tested time points as indicated in both RNA (Fig. 6B middle and right panels) and protein level (Fig. 6C middle and right panels), suggesting that MBP-T12C can work well against OGNNV as low titer as the natural infection.

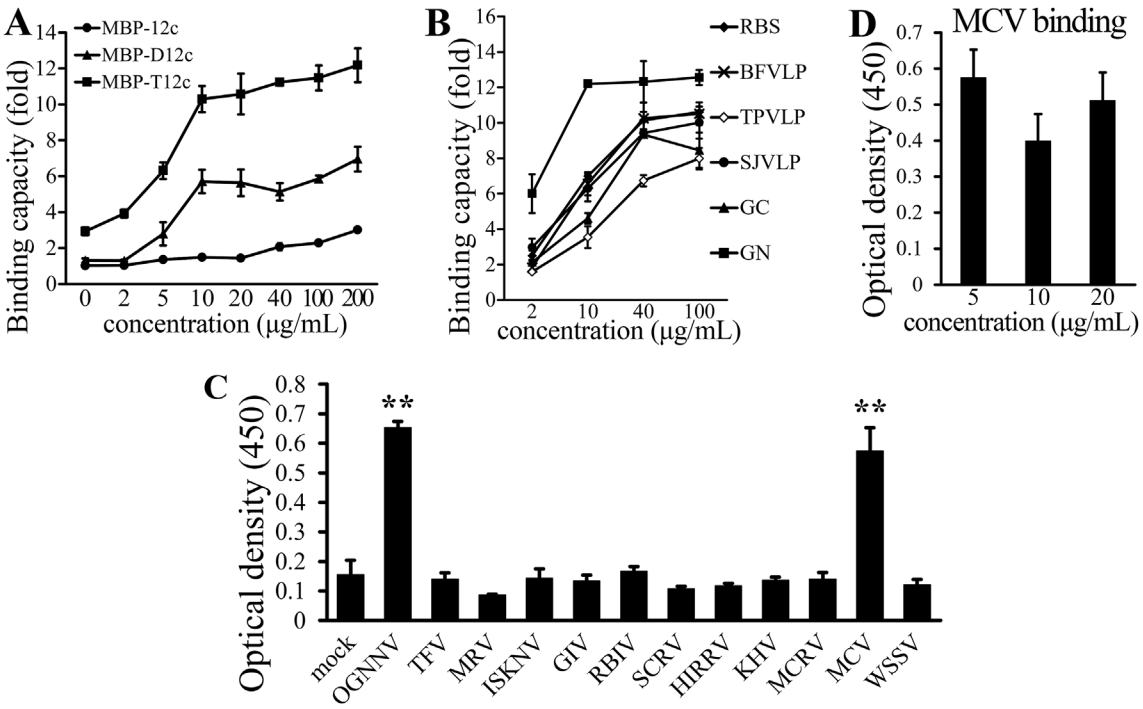

Fig. 4. The BCs of MBP-recombinant proteins detected by ELISA. (A) The BCs of three recombinant proteins for RBS. (B) The BC of MBP-T12C for different serotypes VLPs and CP mutants. (C) Binding specificity of MBP-T12C for different aquatic viruses. Twelve aquatic viruses in easy detectable concentration were used. (**, $p < 0.01$) (D) The BC of MBP-T12C for MCV was not dose-dependent.

4. Discussion

To control NNV infections in adult fish or broodstocks, vaccines based on inactivated viruses or VLPs are viable [31]. However, such vaccines can hardly be used in larvae and juveniles, whose adaptive immune systems are not well developed [8]. For larvae and juveniles, another strategy for the elimination of viral infections is the neutralization of viral particles by natural or chemical compounds [3]. Here, we described a 12-mer AFP (12A) that was screened from phage display peptide libraries using RBS as the target. The amended AFP (12B) hindered RBS entry at low concentration and disrupted the virion at high concentration. This AFP with anti-NNV activity inhibited betanodavirus infection by binding to the virion surface. However, it is far difficult to identify and synthesize naturally generated AMPs than AFPs. AFP-screening techniques, such as phage display libraries, yeast two-hybrid systems, oligopeptide libraries, and bioinformatic design [40], are efficient and user-friendly. The screened AFP candidates can be not only developed as CAIs [30] or conformational inhibitors but also optimized for application in purification [41]. We verified the BC of the AFP 12B, suggesting that a purification method of betanodaviruses or corresponding VLPs based on this peptide deserves further study. Moreover, we identified ANK-GPCR, a protein that may interact with OGNNV as viral receptor candidate, in the grouper genome. According to the ANK-GPCR sequence, we synthesized an additional 12-mer AFP (12C) with higher BC for RBS than 12B.

AFPs generally act to inhibit pathogens via four types of mechanisms: binding to disrupt or destroy protein structure, similar to the neutralizing antibodies; binding to induce slight conformational change without destroying the target protein [40]; binding to coat or envelop the pathogens, forming a lattice structure [12]; and binding to interfere with the assembly of structural proteins [30]. At low concentration, the AFP 12B bound and aggregated RBS, forming a lattice and consequently inhibiting RBS entry. At high concentration, 12B disrupted RBS, indicating that 12B utilize multiple inhibition mechanisms. Furthermore, 12B maintains a high BC for RBS even in high salinities, expanding the scope of 12B usage. It remains unclear whether 12B hinders VLP assembly as a CAI, which deserves further investigation.

By using the strategy of prokaryotic fusion expression and multiple tandem AFP repeats, we increased AFP solubility, enhanced AFP BC, improved AFP production, and simplified AFP purification. As the AFP BC was enhanced, it was necessary to evaluate the binding spectrum and specificity of MBP-T12C [10]. The binding spectrum of MBP-T12C was similar to but broader than that of the anti-RBS antibody. MBP-T12C bound all three serotypes VLPs, with the lowest BC for serotype B (TPVLP), while the anti-RBS antibody did not detect TPVLP. However, the broad-spectrum binding of MBP-T12C should be further verified *in vivo* with several repetitions in different fish species. GN was the preferred target of MBP-T12C, as the BC of MBP-T12C for GN was the highest. This is consistent with strong immunogenicity and high oligopeptide affinity of the CP N + S domain [42]. The well binding specificity of MBP-T12C was also clearly demonstrated by binding test against 11 aquatic viruses. MBP-T12C did not effectively bind with any of these viruses except the positive control, OGNNV, and crab MCV. This suggested that the surface structure of MRV might be highly similar to that of NNV. MCV, a newly-discovered nonenveloped virus causing high mortalities in cultured mud crab, is closely related to nodaviruses, both genetically and structurally [37]. Thus, MBP-T12C might also act as an anti-MCV AFP. However, as the binding of MBP-T12C to MCV was not dose-dependent, the precise binding mechanism between MBP-T12C and MCV should be further examined.

MBP-T12C both hindered RBS entry and inhibited OGNNV infection at viral entry, but did not block viral propagation either by suppressing viral genome replication or by hampering viral protein expression. The inefficient inhibition of OGNNV propagation might be due to the delivery difficulties. Indeed, this is a general problem faced by bioactive molecules [43]. To enhance the antiviral activity of AFPs, cell penetrating peptides (CPPs) have been fused with biologically active proteins [44]. Alternatively, antiviral agents have been wrapped in nanoparticles were, allowing these agents to pass through the cell membrane [45], increasing the in-cell concentration of functional molecules.

In conclusion, a 12-mer AFP screened from phage display peptide libraries blocked RBS entry via virion agglutination and disruption. The

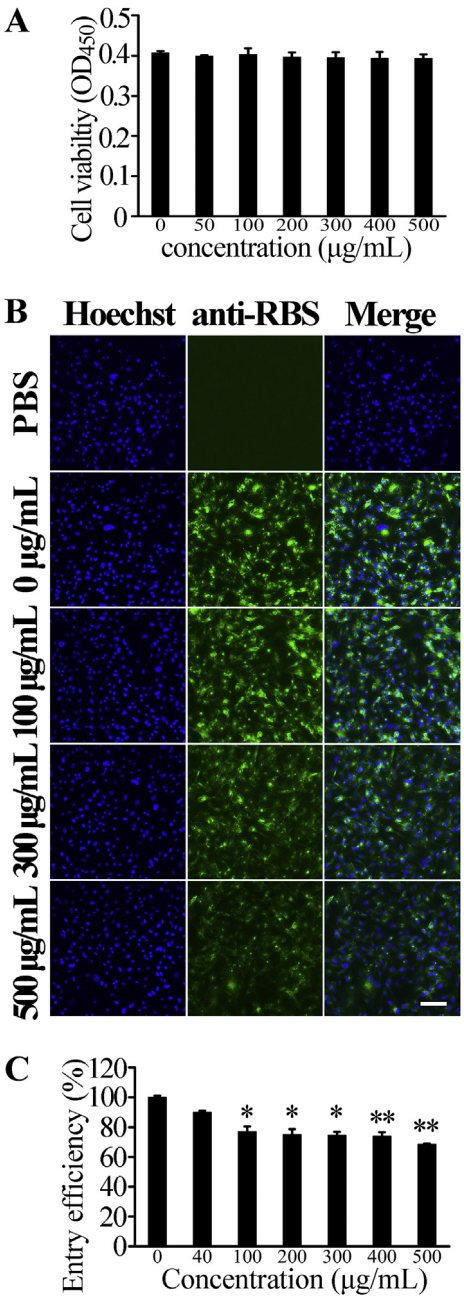

Fig. 5. MBP-T12C inhibited RBS entry. (A) Cytotoxicity of MBP-T12C on SB cells. (B) MBP-T12C strongly inhibited RBS entry detected by IFA. RBS (green) were mixed with different concentrations of MBP-T12C, incubated with SB cells, and detected by IFA. The cell nuclei (blue) were counterstained by Hoechst. The bar indicated 100 μm. (C) MBP-T12C significantly inhibited RBS entry detected by ELISA. (*, $p < 0.05$; **, $p < 0.01$). (For interpretation of the references to colour in this figure legend, the reader is referred to the Web version of this article.)

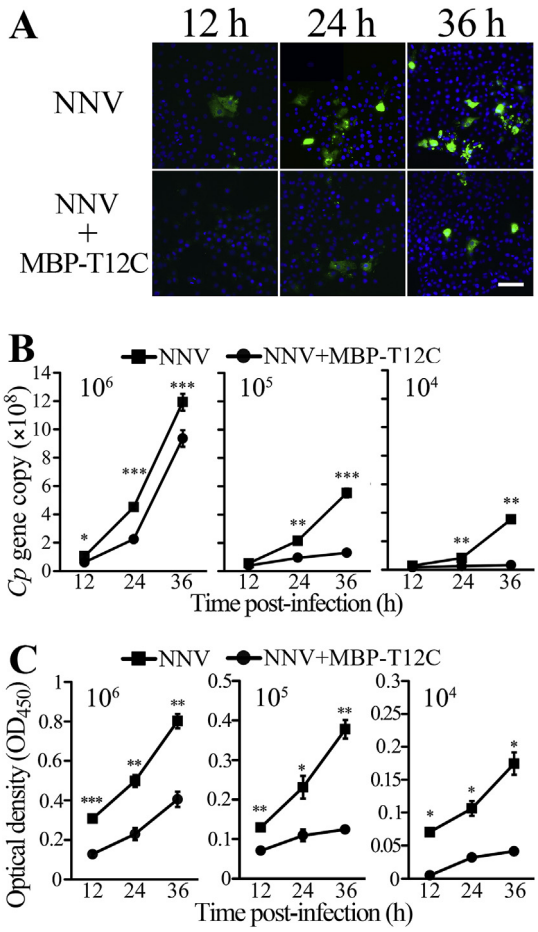

Fig. 6. MBP-T12C neutralized OGNNV to exert antiviral activity on SC1 cell. (A) MBP-T12C (500 μg/mL) strongly neutralized OGNNV (10^6 $TCID_{50}$/mL) to inhibit infection detected by IFA at different time points post-infection. Green signals were OGNNV, and the cell nuclei were counterstained into blue by Hoechst. The bar indicated 100 μm. (B) C*p* gene copies detected by RT-qPCR. (C) CP protein quantities detected by ELISA. At different time points post-infection, RNA level and protein level of MBP-T12C (500 μg/mL) neutralized or untreated OGNNV in different titers (10^4, 10^5, and 10^6 $TCID_{50}$/mL) were determined to indicate viral quantities. Results from all methods showed that MBP-T12C efficiently inhibited OGNNV infection. (*, $p < 0.05$; **, $p < 0.01$; ***, $p < 0.001$). (For interpretation of the references to colour in this figure legend, the reader is referred to the Web version of this article.)

sequence of this AFP was altered according to its homolog in the orange-spotted grouper. The modified AFP was prokaryotically expressed as a triple tandem fusion protein which strongly bound all the NNV serotypes as well as MCV, blocking RBS entry and inhibiting OGNNV infection at the stage of viral entry. This AFP and fusion protein are excellent anti-NNV candidates for application study.

Author contribution

Q Zhou performed all the SDS-PAGE, western blot and ELISA. J Zhang prepared all kinds of the recombinant proteins and VLPs. R Huang performed the cell entry assay and OGNNV infection. S Huang performed TEM and RT-qPCR. Y Wu cultured cells and performed cytotoxicity assay. L Huang performed the phage library screen. J He supervised the work and edited the final version of this manuscript. J Xie designed the study, guided the experiments and edited the final version of this manuscript. All authors read and approved the final manuscript.

Conflicts of interest

The authors declare that they have no competing interests.

Acknowledgment

We thank Dr. Chuanfu Dong, the associate professor of Sun Yat-sen University, for providing the aquatic viruses for binding specificity test. We also thank LetPub (www.letpub.com) for providing linguistic assistance during the preparation of this manuscript. This work was supported by the Science and Technology Planning Project of

Guangdong Province-Public Welfare Research and Capacity Construction Special Project, China (2015B020203001); Special Fund for Fisheries-Scientific Research of Guangdong Province, China (A201600A02, A201501A03, A201400A01, GD2012-B01); Science and Technology Program of Guangzhou, China (201607020014); National Science and Technology Pillar Program, China (No. 2012BAD17B02, 2011BAD13B11, 2007BAD 29B05); Fundamental Research Funds for the Central Universities of China (No. 11lgpy81); State Scholarship Fund of the China Scholarship Council (CSC) (No. 2008109931).

Appendix A. Supplementary data

Supplementary data related to this article can be found at https://doi.org/10.1016/j.fsi.2018.12.003.

References

[1] T. Nakai, K. Mori, T. Sugaya, T. Nishioka, K. Mushiake, H. Yamashita, Current knowledge on viral nervous necrosis (VNN) and its causative betanodaviruses, Israeli J. Aquacult. – Bamidgeh 61 (2009) 198–207.
[2] J.Z. Costa, K.D. Thompson, Understanding the interaction between Betanodavirus and its host for the development of prophylactic measures for viral encephalopathy and retinopathy, Fish Shellfish Immunol. 53 (2016) 35–49.
[3] Q.K. Doan, M. Vandeputte, B. Chatain, T. Morin, F. Allal, Viral encephalopathy and retinopathy in aquaculture: a review, J. Fish. Dis. 40 (5) (2017) 717–742.
[4] B. Munday, T. Nakai, Nodaviruses as pathogens in larval and juvenile marine finfish, World J. Microbiol. Biotechnol. 13 (4) (1997) 375–381.
[5] A.M.Q. King, M.J. Adams, E.B. Carstens, E.J. Lefkowitz, Virus Taxonomy: Classification and Nomenclature of Viruses. Ninth Report of the International Committee on Taxonomy of Viruses, Elsevier Academic Press, London, San Diego, 2011.
[6] R. Huang, Q. Zhou, Y. Shi, J. Zhang, J. He, J. Xie, Protein A from orange-spotted grouper nervous necrosis virus triggers type I interferon production in fish cell, Fish Shellfish Immunol. 79 (2018) 234–243.
[7] B.J. Fenner, R. Thiagarajan, H.K. Chua, J. Kwang, Betanodavirus B2 is an RNA interference antagonist that facilitates intracellular viral RNA accumulation, J. Virol. 80 (1) (2006) 85–94.
[8] C.F. Low, B. Syarul Nataqain, H.Y. Chee, M.Z.H. Rozaini, M. Najiah, Betanodavirus: dissection of the viral life cycle, J. Fish. Dis. 40 (11) (2017) 1489–1496.
[9] K. Morit, T. Mangyoku, T. Iwamoto, M. Arimoto, S. Tanaka, T. Nakai, Serological relationships among genotypic variants of betanodavirus, Dis. Aquat. Org. 57 (1–2) (2003) 19–26.
[10] F. Pascoli, A. Guazzo, A. Buratin, M. Toson, F. Buonocore, G. Scapigliati, A. Toffan, Lack of *in Vivo* Cross-protection of Two Different Betanodavirus Species RGNNV and SJNNV in European Sea Bass *Dicentrachus Labrax*, Fish Shellfish Immunol, 2017.
[11] L. Y-S, C. H-C, M. S, G. I-C, C. S-C, F. K, C. C-Y, In vitro neutralization by monoclonal antibodies against yellow grouper nervous necrosis virus (YGNNV) and immunolocalization of virus infection in yellow grouper, *Epinephelus awoara* (Temminck & Schlegel), J. Fish. Dis. 24 (4) (2001) 237–244.
[12] T.J. Chia, Y.C. Wu, J.Y. Chen, S.C. Chi, Antimicrobial peptides (AMP) with antiviral activity against fish nodavirus, Fish Shellfish Immunol. 28 (3) (2010) 434–439.
[13] Y.D. Wang, C.W. Kung, J.Y. Chen, Antiviral activity by fish antimicrobial peptides of epinecidin-1 and hepcidin 1-5 against nervous necrosis virus in medaka, Peptides 31 (6) (2010) 1026–1033.
[14] L. Zhou, P. Li, M. Yang, Y. Yu, Y. Huang, J. Wei, S. Wei, Q. Qin, Generation and characterization of novel DNA aptamers against coat protein of grouper nervous necrosis virus (GNNV) with antiviral activities and delivery potential in grouper cells, Antivir. Res. 129 (2016) 104–114.
[15] Y.C. Huang, Y.S. Han, Determining anti-betanodavirus compounds through a GF-1 cell-based screening platform, Antivir. Res. 105 (2014) 47–53.
[16] K.A. Brogden, M. Ackermann, P.B. McCray Jr., B.F. Tack, Antimicrobial peptides in animals and their role in host defences, Int. J. Antimicrob. Agents 22 (5) (2003) 465–478.
[17] Z.-X. Yin, W. He, W.-J. Chen, J.-H. Yan, J.-N. Yang, S.-M. Chan, J.-G. He, Cloning, expression and antimicrobial activity of an antimicrobial peptide, epinecidin-1, from the orange-spotted grouper, *Epinephelus coioides*, Aquaculture 253 (1) (2006) 204–211.
[18] M. Guo, J. Wei, X. Huang, Y. Huang, Q. Qin, Antiviral effects of beta-defensin derived from orange-spotted grouper (*Epinephelus coioides*), Fish Shellfish Immunol. 32 (5) (2012) 828–838.
[19] A.M. Cole, P. Weis, G. Diamond, Isolation and characterization of pleurocidin, an antimicrobial peptide in the skin secretions of winter flounder, J. Biol. Chem. 272 (18) (1997) 12008–12013.
[20] P.H. Huang, J.Y. Chen, C.M. Kuo, Three different hepcidins from tilapia, *Oreochromis mossambicus*: analysis of their expressions and biological functions, Mol. Immunol. 44 (8) (2007) 1922–1934.
[21] A. Cuesta, J. Meseguer, M.A. Esteban, The antimicrobial peptide hepcidin exerts an important role in the innate immunity against bacteria in the bony fish gilthead seabream, Mol. Immunol. 45 (8) (2008) 2333–2342.
[22] D.C. Broekman, A. Zenz, B.K. Gudmundsdottir, K. Lohner, V.H. Maier, G.H. Gudmundsson, Functional characterization of codCath, the mature cathelicidin antimicrobial peptide from Atlantic cod (*Gadus morhua*), Peptides 32 (10) (2011) 2044–2051.
[23] Z.-r. Zhuang, X.-d. Yang, X.-z. Huang, H.-x. Gu, H.-y. Wei, Y.-j. He, L. Deng, Three new piscidins from orange-spotted grouper (*Epinephelus coioides*): phylogeny, expression and functional characterization, Fish Shellfish Immunol. 66 (2017) 240–253.
[24] I. Mulero, E.J. Noga, J. Meseguer, A. Garcia-Ayala, V. Mulero, The antimicrobial peptides piscidins are stored in the granules of professional phagocytic granulocytes of fish and are delivered to the bacteria-containing phagosome upon phagocytosis, Dev. Comp. Immunol. 32 (12) (2008) 1531–1538.
[25] S. Rakers, L. Niklasson, D. Steinhagen, C. Kruse, J. Schauber, K. Sundell, R. Paus, Antimicrobial peptides (AMPs) from fish epidermis: perspectives for investigative dermatology, J. Invest. Dermatol. 133 (5) (2013) 1140–1149.
[26] H. Xie, J. Wei, Q. Qin, Antiviral function of Tachyplesin I against iridovirus and nodavirus, Fish Shellfish Immunol. 58 (2016) 96–102.
[27] R.E. Hancock, A. Rozek, Role of membranes in the activities of antimicrobial cationic peptides, FEMS Microbiol. Lett. 206 (2) (2002) 143–149.
[28] J.J. Oppenheim, A. Biragyn, L.W. Kwak, D. Yang, Roles of antimicrobial peptides such as defensins in innate and adaptive immunity, Ann. Rheum. Dis. 62 (Suppl 2) (2003) ii17–21.
[29] O. Chertov, D.F. Michiel, L. Xu, J.M. Wang, K. Tani, W.J. Murphy, D.L. Longo, D.D. Taub, J.J. Oppenheim, Identification of defensin-1, defensin-2, and CAP37/azurocidin as T-cell chemoattractant proteins released from interleukin-8-stimulated neutrophils, J. Biol. Chem. 271 (6) (1996) 2935–2940.
[30] J. Sticht, M. Humbert, S. Findlow, J. Bodem, B. Muller, U. Dietrich, J. Werner, H.G. Krausslich, A peptide inhibitor of HIV-1 assembly *in vitro*, Nat. Struct. Mol. Biol. 12 (8) (2005) 671–677.
[31] Y.X. Lai, B.L. Jin, Y. Xu, L.J. Huang, R.Q. Huang, Y. Zhang, J. Kwang, J.G. He, J.F. Xie, Immune responses of orange-spotted grouper, *Epinephelus coioides*, against virus-like particles of betanodavirus produced in *Escherichia coli*, Vet. Immunol. Immunopathol. 157 (1–2) (2014) 87–96.
[32] J. Xie, K. Li, Y. Gao, R. Huang, Y. Lai, Y. Shi, S. Yang, G. Zhu, Q. Zhang, J. He, Structural analysis and insertion study reveal the ideal sites for surface displaying foreign peptides on a betanodavirus-like particle, Vet. Res. 47 (2016) 16.
[33] C. Dong, Z. Wang, S. Weng, J. He, Occurrence of a lethal ranavirus in hybrid Mandarin (*Siniperca scherzerixSiniperca chuatsi*) in Guangdong, South China, Vet. Microbiol. 203 (2017) 28–33.
[34] H. Qi, Y. Yi, S. Weng, W. Zou, J. He, C. Dong, Differential autophagic effects triggered by five different vertebrate iridoviruses in a common, highly permissive mandarinfish fry (MFF-1) cell model, Fish Shellfish Immunol. 49 (2016) 407–419.
[35] C. Dong, X. Li, S. Weng, S. Xie, J. He, Emergence of fatal European genotype CyHV-3/KHV in mainland China, Vet. Microbiol. 162 (1) (2013) 239–244.
[36] X.X. Deng, L. Lu, Y.J. Ou, H.J. Su, G. Li, Z.X. Guo, R. Zhang, P.R. Zheng, Y.G. Chen, J.G. He, S.P. Weng, Sequence analysis of 12 genome segments of mud crab reovirus (MCRV), Virology 422 (2) (2012) 185–194.
[37] J. Huang, Identification and Tissue Distribution of a New Mud Crab Virus, Master thesis of Sun Yat-sen University, 2018.
[38] Z.Y. Zhao, Z.X. Yin, X.P. Xu, S.P. Weng, X.Y. Rao, Z.X. Dai, Y.W. Luo, G. Yang, Z.S. Li, H.J. Guan, S.D. Li, S.M. Chan, X.Q. Yu, J.G. He, A novel C-type lectin from the shrimp *Litopenaeus vannamei* possesses anti-white spot syndrome virus activity, J. Virol. 83 (1) (2009) 347–356.
[39] R. Huang, G. Zhu, J. Zhang, Y. Lai, Y. Xu, J. He, J. Xie, Betanodavirus-like particles enter host cells via clathrin-mediated endocytosis in a cholesterol-, pH- and cytoskeleton-dependent manner, Vet. Res. 48 (1) (2017) 8.
[40] R.U. Kadam, J. Juraszek, B. Brandenburg, C. Buyck, W.B.G. Schepens, B. Kesteleyn, B. Stoops, R.J. Vreeken, J. Vermond, W. Goutier, C. Tang, R. Vogels, R.H.E. Friesen, J. Goudsmit, M.J.P. van Dongen, I.A. Wilson, Potent peptidic fusion inhibitors of influenza virus, Science 358 (6362) (2017) 496–502.
[41] Y. Li, X. Liu, X. Dong, L. Zhang, Y. Sun, Biomimetic design of affinity peptide ligand for capsomere of virus-like particle, Langmuir 30 (28) (2014) 8500–8508.
[42] N.C. Chen, M. Yoshimura, H.H. Guan, T.Y. Wang, Y. Misumi, C.C. Lin, P. Chuankhayan, A. Nakagawa, S.I. Chan, T. Tsukihara, T.Y. Chen, C.J. Chen, Crystal structures of a piscine betanodavirus: mechanisms of capsid assembly and viral infection, PLoS Pathog. 11 (10) (2015) e1005203.
[43] S.R. Schwarze, A. Ho, A. Vocero-Akbani, S.F. Dowdy, In vivo protein transduction: delivery of a biologically active protein into the mouse, Science 285 (5433) (1999) 1569–1572.
[44] G. Elliott, P. O'Hare, Intercellular trafficking and protein delivery by a herpesvirus structural protein, Cell 88 (2) (1997) 223–233.
[45] H.P. Kuo, L.L. Goh, M.W. Lu, Z.L. Kong, Delivery of grouper interferon by chitosan-modified poly(lactic-co-glycolic acid) nanoparticles to protect nervous necrosis virus infection, J. Nanosci. Nanotechnol. 16 (7) (2016) 7521–7529.